Chapter III Randomly Functionalized Linear Chains with Complementary Groups

3.1 Introduction

Previously we saw that for solutions of self-associating chains (Figure 1.7.1), intrachain pairing is more important than interchain pairing, even up to concentrations $c >> c^*$. In dilute solutions, the addition of self-associating stickers leads to chain collapse and reduces the effect of the polymer on drop breakup. To drive intermolecular associations in dilute solutions,[1] strategies involving the use of complementary functional groups were designed (Figure 1.7.2). In this chapter we study the association behavior of mixtures of tertiary amine and carboxylic acid-functionalized 1,4-polybutadiene chains of size M_w = 1250 kg/mol (Scheme 3.1).

3.1.1 Background

A review of the literature reveals that mixtures of two different linear chain species, one randomly functionalized with hydrogen-bond donating groups and the other with hydrogen-bond accepting groups, exhibit the following behaviors: First, donor and acceptor chains form clusters of increasing size with increasing concentration, even below c^*, and the resulting interpolymer complexes have been reported to exhibit improved shear stability as well as enhanced drag-reduction properties.[2] Second, intermolecular associations nevertheless result in some measure of chain collapse, as well as in non-linear enhancements in shear viscosity with increasing concentration. Here we give a brief literature review of the above and of other relevant behavior of hydrogen donor-acceptor systems, and discuss implications for the design of successful mist-suppression additives.

Donor-acceptor intermolecular associations can cause aggregation of polymer molecules well below the overlap concentration. Malik and Mashelkar[3] investigated the solution properties of blends of poly(dodecyl acrylate-co-methacrylic acid) (DAMA, 3 wt % methacrylic acid) and poly(styrene-co-dodecyl acrylate-co-4-vinyl pyridine) (PSDAVP, 4 wt % vinyl pyridine) (Figure 1.5.b) in kerosene. Using dynamic light scattering, they observed the formation of interpolymer complexes (IPC) whose size increased steeply with increasing polymer concentration near the overlap concentration c^* (see Figure 3.1). Note that

interpolymer complexes at c = 0.3 g/dL were one order of magnitude larger than the component polymers.

Jian and coworkers[4] studied the complexation of poly(styrene-co-vinylphenol) (STVPh) and poly(styrene-co-vinylpyridine) (STVPy) in organic solvents by viscometry and dynamic laser light scattering. They observed the formation of aggregates ~ 1 order of magnitude larger (in hydrodynamic radius R_h) than the individual polymer coils in very dilute blend solutions in both butanone and tetrahydrofuran. (The butanone case is shown in Figure 3.2.)

It should be noted that the observation of interpolymer aggregates in the dilute concentration regime supports the prediction that the strength of the acid-base interaction dwarfs the strength of self-association of the carboxylic acid donor groups via dimerization.

Interpolymer complexation results in a contraction of the polymer chains, causing a decrease in the specific viscosity of the blends compared to that of the component polymer solutions at the same concentration. Jiang and coworkers[4] used viscosity measurements in dilute solutions to evaluate the effect of sticker density (i.e., number density of interacting groups) on complex formation for blends of STVPh and STVP. Large negative deviations in specific viscosity from predicted values for non-associating polymer systems were observed in the dilute regime, indicating coil contraction due to the formation of dense intermolecular complexes (see Figure 3.3). For non-interacting polymer molecules, the specific viscosity $\eta_{sp,m,calc}$ of a ternary polymer$_1$-polymer$_2$-solvent system is simply a weighted average of the specific viscosities of both components:

$$\eta_{sp,m,calc} = \left(\eta_{sp,1}c_1 + \eta_{sp,2}c_2\right)\Big/c_m \tag{3.1}$$

where $\eta_{sp,1}$, $\eta_{sp,2}$ are the specific viscosities of components 1 and 2 at concentration $c_m = c_1 + c_2$. According to Equation 3.1, the reduced viscosity of a non-interacting polymer system would thus exhibit a linear variation from x = 0 to x = 1 in Figure 3.3. For a given value of the x-coordinate (say 0.5), the number density in solution of hydrogen-accepting moieties is fixed while the number density of hydrogen-donating moieties increases as we move down from one curve to the next (i.e., with increasing fraction of vinylphenol in STVPh). As one might expect, this results in an increase in polymer complexation, and specifically in an increase in the number density of paired stickers within the aggregates. The pronounced negative deviation in observed reduced viscosity for the bottom 3 curves in Figure 3.3 is easily understood in terms of a collapse of the coils as polymer molecules aggregate into

more and more compact structures (as the number density of H-bonds between donor and acceptor polymer molecules increases.) In other words, the polymers are making a much smaller contribution to the solution viscosity in the form of collapsed aggregates than in the form of swollen coils.

Wang et al. reported a similar phenomenon for blends of poly(styrene-co-octyl acrylate-co-acrylic acid) and poly(styrene-co-octyl acrylate-co-4-vinylpyridine) in toluene.[5-7] For dilute blends, they observed negative deviations in the measured specific viscosity of the mixture $\eta_{sp,m,exp}$ from the expected value $\eta_{sp,m,calc}$ for non-interacting systems, indicating a reduction in the hydrodynamic volume fraction occupied by the polymer molecules in solution. This was attributed to the aggregation of polymer chains into dense structures as a result of intermolecular associations.

Interpolymer associations result in a non-linear increase of viscosity with concentration even in the dilute concentration regime. Intermolecular interactions make two kinds of contributions to the specific viscosity of solutions of associating polymer systems. In very dilute solutions of strongly associating polymer, negative deviations from the additivity rule (Equation 3.1) are observed due to the aggregation of constituent polymer molecules into relatively compact structures of high physical crosslink density, as observed by Jiang et al.[4, 8, 9] and Wang et al.[5-7] As concentration increases, these compact structures begin to interact, and eventually to form a reversible network, giving rise to a large positive deviation from the value predicted by Equation 3.1. Therefore, due to intermolecular associations, the concentration dependence of reduced viscosity is curved even at very low polymer concentrations (Figure 3.4).

Other solution behavior of donor-acceptor polymer mixtures relevant to mist inhibition applications. As expected, the nature of the solvent exerts a profound influence on interpolymer association. In particular, for polymer interactions based on hydrogen bonding or acid-base interactions, the hydrogen-bonding ability of the solvent has a pronounced effect on the extent of association. For instance, Jiang et al.[4] observed much more pronounced negative deviations in the reduced viscosity of STVPh/STVPy mixtures in $CHCl_3$ than in tetrahydrofuran (THF), even at considerably smaller number density of stickers. This is consistent with a strong competition for H-bonding from the solvent in THF, which reduces

the fraction of the total H-bonds that contribute to complex formation and the physical crosslink density within the aggregates.

In spite of the above understanding, survey of the literature reveals that there is nevertheless little comprehension of the precise structure of interpolymer complexes *at the molecular level*, or of the relationship between molecular or aggregate structure and rheological properties or performance in drop breakup or drag reduction.

Design principles for donor-acceptor associative polymers as mist-control agents. In order to minimize the effects of chain collapse as well as minimize shear viscosity enhancements, future work should focus on polymer molecules with low extents of functionalization with associative groups, and in dilute solutions at concentrations $c < c^*$. The above literature results generate optimism that under these conditions, donor-acceptor specific interactions can be used to achieve formation of large clusters which protect against mechanical degradation and greatly increase extentional viscosity, but only slightly increase shear viscosity.

3.1.2 Scope of Present Work

What part of the variable space should we endeavor to study? Solution behavior will depend on at least the following parameters: solvent, chain lengths, temperature, extents of functionalization of donor and acceptor chains, and concentrations of donor and acceptor chains in solution. In this chapter we restrict our attention to systems which might lead us to a suitable additive for improving the fire safety of jet fuel.

The choice of solvent has such strong effects on the solubility of the functional polymers and their complexes[4,10] that it is necessary to perform experiments using the solvent of interest, here Jet-A. The choice of chain lengths of interest for use in fuel are limited to values that are long enough to confer significant elasticity and short enough to avoid chain scission at high shear rates. We know that the elasticity of solutions of 510 kg/mol and 1250 kg/mol PB chains was too low to be quantitatively measured by CaBER at concentrations below 2 wt % and 1.5 wt % (corresponding to $c \sim 4–6\ c^*$) in low-viscosity hydrocarbon solvents. Therefore, studies of the effect of stickers on elasticity of dilute solutions would benefit from the use of longer chains (recall the strong effect of chain length on elasticity).[11] Unfortunately, MW ~ 1×10^6 g/mol represents the upper limit of chain length for molecules

that resist shear degradation. Therefore, the 1250 kg/mol 1,4-PB chains used in the previous study were used again here. To simplify the task of uncovering the effects of the degrees of functionalization of donor and acceptor chains, of the overall polymer concentration, and of the ratio of donor and acceptor chains, we performed experiments holding temperature fixed (i.e., at room temperature).

3.2 Experimental

3.2.1 Materials

2-(Dimethylamino)ethanethiol hydrochloride (DMAET) was obtained at 95% purity from Aldrich. The 510 kg/mol polybutadiene (510kPB prepolymer), the 1250 kg/mol polybutadiene (1250kPB prepolymer), and all other reagents were obtained and purified as described in the preceding chapter (Section 2.2.1).

3.2.2 Polymer Synthesis and Characterization

The functionalization of 510kPB and 1250kPB with DMAET was performed according to the following representative procedure. To 1250kPB (0.50 g, 0.74 mmol 1,2-PB repeat units) dissolved in 50 mL of THF in a 100 mL Schlenk flask were added DMAET (0.31 g, 2.1 mmol) and azobisisobutyronitrile (AIBN, 51 mg, 0.31 mmol), both dissolved in a mixture of 5 mL THF and 5 mL methanol. The contents of the Schlenk flask were degassed in 3 freeze-pump-thaw cycles, warmed to 55 ºC, and then allowed to react at 55 ºC for 7 hrs. Following the reaction, the polymer solution was transferred to a 100 mL jar containing a small amount of 2,6-di-*tert*-butyl-4-methylphenol (BHT), concentrated by evaporation of all but the last 20 mL solvent under an argon stream, and titrated by addition of potassium hydroxide (0.31 g at 88%, 4.9 mmol, dissolved in a ~1:3:6 water:methanol:THF solution). The solution was cooled in liquid nitrogen and precipitated by addition of 50 mL of cold methanol. Final purification of the polymer was achieved by reprecipitating from a THF solution (containing ca. 1 wt % BHT) once with 50:50 methanol:water, and once again with cold methanol, followed by drying to constant weight under vacuum at room temperature. Reaction conditions and results are summarized in Tables 3.1 and 3.2, and results of product characterization by ^{1}H NMR and GPC are shown in Figures 3.5 and 3.6.

Acid-functionalized 1250 kg/mol 1,4-PB chains used in this study were the same as those used in earlier studies (Section 2.3.1, Table 3.1). The characterization of functionalized

polymer by gel permeation chromatography and ^{1}H NMR was performed as documented previously (Section 2.2.3).

3.2.3 Measurements of Solution Properties

Dilute mixtures of acid-functionalized and amine-functionalized polymer were prepared from stock solutions of the individual polymers by mixing in appropriate ratios to obtain target concentrations. The zero-shear viscosity, apparent hydrodynamic size of polymer clusters, and the fluid break-up and atomization of the solutions were characterized as described in Chapter 2 (Sections 2.2.4 and 2.2.5).

3.3 Results and Discussion

3.3.1 Synthesis of Amine-Functionalized Polybutadiene

Reaction of 1,4-PB (Scheme 3.1) using the procedure outlined in Section 3.2.2 successfully incorporates tertiary amine side-groups (Table 3.1, Figure 3.5). Unfortunately, we were not able to assess the MW distribution of the resultant amine-functionalized 1250kPB by gel permeation chromatography using our instrument: at every injection the RI detector output featured the absence of a polymer peak. Note that this anomalous behavior has been observed in other cases, for example with phenol-functionalized 92 kg/mol 1,2-PB (entry 92kPB12 in Table 5.1). Given that the addition of DMAET to 1,2-PB (using the same procedure) and the addition of 3-mercaptopropionic acid (MPA) to 1,4-PB both proceed without degradation of the polymer backbone (Tables 3.1 and 3.2, Figures 2.4 and 3.6), it is reasonable to expect that the narrow polydispersity of the 1250kPB starting material was also preserved during the addition reaction of DMAET. This is consistent with the result that the viscosities of 1250k1.5N and 1250kPB polymers were identical at the overlap concentration of 2500 ppm in Jet-A (Figure 3.7). For 1250kPB2.6N and 1250kPB5.4N polymers, however, appreciable viscosity enhancements compared to the prepolymer material (Figure 3.7) suggests that a small amount of crosslinking of the polymer occurred, presumably during the workup stage of the preparation of the materials.

3.3.2 Phase Behavior

The degree of functionalization was restricted to be low enough that the individual species dissolve to form homogenous solutions in Jet-A at 25 ºC at all concentrations tested

(up to 1.5 wt % polymer). As a result, the highest degrees of functionalization utilized in this study were 5.4 tertiary amine side-groups per 100 butadiene units, and 0.6 carboxylic acid side-groups per 100 butadiene units (Table 3.1). Nevertheless, intermolecular associations of carboxylic acid and tertiary amine side-groups were found to promote phase separation into polymer-rich (gel) and polymer-poor (sol) phases (Table 3.3). Phase behavior was a strong function of temperature. For example, 1250kPB0.6A polymer separated into gel and sol phases in Jet-A at 0 ºC at all concentrations tested.

We chose to conduct further examination of solution properties only for those pairs of polymers in Table 3.3 that did not yield phase separation. A summary of further experiments is given in Table 3.4.

3.3.3 Aggregate Formation and Effects on Shear Viscosity

Upon inspection of shear viscosity results at the overlap concentration of the 1250kPB chains (corresponding to c^* = 2500 ppm by wt in Jet-A for the unfunctionalized chains, Figure 3.7), we immediately observe an important difference between non-specific, pair-wise self-associations, and specific, donor-acceptor interactions: at that concentration for all the molecules studied, self associations led to negative deviations in η_0 (look at the acid-functionalized molecules by themselves), but interchain donor-acceptor associations led to positive deviations in η_0. This indicates that in the self-associating case, the effects of chain collapse dominate over any positive enhancement in shear viscosity due to formation of polymer clusters; in the donor-acceptor case the opposite holds.

Measuring polymer aggregation in terms of particle size can be readily achieved by dynamic light scattering. Results at 1500 ppm (Figure 3.8) validate our expectations that donor-acceptor interactions can "force" polymer chains to associate even in dilute solutions. At intermediate compositions, objects with hydrodynamic size greater than either individual components are observed. At this dilute condition, self-associating stickers do not cause the acid-functionalized molecules to form large aggregates. Increasing polymer concentration to c^* increases the size of interpolymer complexes (Figures 3.9 and 3.10), in good agreement with literature reports on similar systems (discussed earlier). Large increases in $\langle R_h \rangle$ can be achieved at concentrations as low as c^*: for example, a 3-fold increase in hydrodynamic radius could be obtained at c^* = 2500 ppm for mixtures of 1250kPB0.2A and 1250kPB5.4N (Figure 3.9).

For fixed sticker density on one partner (e.g., 1.5% N), increasing the sticker density on the other partner leads to larger aggregates, at least up to the limit imposed by phase separation. Notice that phase separation precludes simply increasing sticker density on both species as a means to promote larger aggregates. At a certain point, further increases of number density of stickers on one of the chains requires a reduction of the number density of stickers on the partner chains in order to remain in the homogeneous regime. We found that the largest aggregates form when the extent of functionalization of one of the species is pushed up to its single-component solubility limit. Thus, mixtures of 1250kPB0.2A and 1250kPB5.4N polymers, and mixtures of 1250kPB0.8A and 1250kPB1.5N polymers gave the highest enhancement in $\langle R_h \rangle$ at both 1500 and 2500 ppm (Figures 3.8 and 3.9).

For a given pair of acid-functionalized and base-functionalized polymer, we further observe that the largest clusters were obtained in the vicinity of 1:1 weight ratios of the chains, in some cases far from 1:1 molar ratios of the stickers. This very interesting result held for all mixtures tested at both 1500 and 2500 ppm (Figures 3.8 and 3.9).

We close this section by commenting on the relative magnitude of the changes in $\langle R_h \rangle$ and η_0 as a result of interpolymer associations. Except for the mixture involving 1250kPB5.4N, which is measurably crosslinked, deviations in η_0 due to interchain associations were < 20% at the overlap concentration of 2500 ppm (Figure 3.7), compared with up to 300% changes in $\langle R_h \rangle$ (Figure 3.9). It is noteworthy that cluster size is not a good indicator of viscosity enhancements. Indeed, in the following section we find that these large clusters provide no observable enhancements of the elasticity or mist-suppression capacity of the solutions in extensional deformation—contrary to expectations based on the prior literature.

If the concentration is increased in order to confer elasticity to the solutions (and thereby, suppress misting), strong increases of shear viscosity also occur (which hinder application of such solutions in fuel systems). In the following investigation of elasticity and mist suppression, concentrations of 15,000 ppm (1.5 wt %) were required for successful CaBER measurements (see below). At such high concentration, the shear viscosity in donor-acceptor mixtures is increased 2- to 3-fold relative to controls with unfunctionalized polymer or the individual functionalized species. For example, mixtures of 1250kPB2.6N and 1250kPB0.2A in 15:85 and 30:70 wt ratios at total polymer concentrations of 1.5 wt % in

Jet-A were 130 and 180 mPa.s, respectively, compared with 48, 62, and 77 mPa.s for 1250kPB prepolymer, 1250kPB0.2A, and 1250kPB2.6N individual polymers at 1.5 wt % in Jet-A.

3.3.4 Elasticity and Mist Suppression

Drop impact experiments enable us to evaluate the effect of donor-acceptor associations on solution elasticity and drop breakup in very dilute solutions (Figure 3.11). Recall[12] that fluid filaments do not break when 180 ppm of 4200 kg/mol linear PIB are dissolved in Jet-A: the fluid filaments seen in Figure 3.11a simply fall down onto the surface. When chain length is reduced into a range that would survive shear degradation, then substantial fluid is ejected: with 180 ppm of 1250 kg/mol PB, the fluid filaments elongate and some drops escape, which are substantially larger than those ejected from pure Jet-A (Figure 2.1), as a result of polymer elasticity. When stickers are present (Figure 3.11c and 3.11d), there is little evidence of fluid filaments, and numerous, fine droplets are ejected in a manner that resembles Jet-A with no polymer added (Figure 2.1). Thus, donor-acceptor interactions do not overcome the limitations found in self-associating systems (Chapter 2). In fact, the mist-suppression performance of the mixture of acid- and base-functionalized polymers was significantly worse than that of the acid-functionalized polymers by themselves (compare with Figure 2.11). Increasing polymer concentration to 450 ppm (Figure 3.12) does not change this finding: while drop suppression improves for all four systems as a result of increased polymer content, the incorporation of associative groups (c–d) still reduces efficacy relative to the unmodified polymer (b) by a factor of 2-4. Note that the poorest performance in suppression of drop breakup corresponds to the largest extent of interpolymer interactions, at 1:1 wt ratio of the chains (Figures 3.7–3.9).

The above results for dilute solutions of donor-acceptor chains cannot a priori be generalized to more concentrated solutions: physical properties for these systems display a strong concentration dependence in the transition between the dilute and semi-dilute regimes. As noted earlier, the drop impact experiment is not informative near c^*. To compare the effects of interpolymer complexes formed near the overlap concentration to their non-associating parent linear chains, spray experiments were conducted on the mixtures whose viscosity and size measurements are given in Figures 3.7 and 3.9. No large differences in atomization could be discerned as a result of donor-acceptor interpolymer associations at c^*

= 2500 ppm (Figures 3.13–3.18). This was true despite the documented presence of aggregates of hydrodynamic radius up to 3 times that of the unfunctionalized chains (Figure 3.9). In fact, in most cases, the size distribution of droplets generated in the spray experiment shifted to smaller values as a result of interpolymer complexation, as was the case for self-associating polymer systems (Figure 2.13).

To place the above qualitative effects on a more rigorous foundation, quantitative measurements of extensional viscosity and relaxation time were performed using capillary breakup rheology. As mentioned in Chapter 2, solution elasticity was unfortunately too low to be measured for 1250 kg/mol 1,4-PB chains at concentrations below 1.5 wt % (corresponding to $c = 6c^*$) in Jet-A solvent.[13] CaBER results for mixtures of 1250kPB0.2A and 1250kPB2.6N polymers at 1.5 wt % show that intermolecular complexation increased solution relaxation time, apparent extensional viscosity, and breakup time of the filaments (Figures 3.19 and 3.20). However, these increases matched precisely the increases in the shear viscosity of the solutions. Thus, intermolecular complexation did not result in significant improvements of the solutions' extensional viscosity or elasticity, relative to shear viscosity, even well into the semi-dilute concentration regime!

Our above observations of the effects of donor-acceptor polymer-polymer interactions on drop and capillary breakup are surprising in light of literature evidence[1, 3, 14] that interpolymer complexation drives the formation of large aggregates and results in enhanced viscosity, shear-thickening rheology, and enhanced drag-reduction (relative to non-associating and self-associating molecules). Based on the positive correlation between drag-reduction and mist-suppression, and on the positive correlation between polymer size and mist suppression, the adverse effects of interpolymer complexation on drop breakup at $c \leq c^*$—in the presence of large polymer structures—is the opposite of what we expected according to the state of prior understanding. These adverse effects indicate that, in the absence of a macroscopic network at low polymer concentrations, interchain associations, like intrachain associations, hinder the mechanism of mist-suppression. We suggest this occurs as physical bonds inhibit stretching of the chains in extensional flow. This physical phenomenon persists at higher concentrations: in spite of large enhancements in shear viscosity (relative to both unfunctionalized and self-associating chains of the same length) in the semi-dilute regime, to our surprise donor-acceptor molecules showed no improvement in relaxation time or extensional viscosity relative to shear viscosity up to $c = 6c^*$ (Figures 3.19 and 3.20).

3.4 Conclusions

We find that the use of complementary associative groups randomly placed along linear polymer chains (Figure 1.7.2, Scheme 3.1) successfully drives intermolecular interactions even in dilute solutions. However, complementary donor-acceptor stickers, like self-associating stickers, decrease the mist-suppression activity of the polymer chains in dilute solutions at polymer concentrations up to the overlap concentration of linear non-associating chains of the same length. At high concentration, associations increase the shear viscosity relative to the unfunctionalized chains; high viscosity suppresses fluid breakup, but is unacceptable in fuel applications.

Our discoveries thus far lead away from randomly functionalized polymers. In light of the results presented in the foregoing two chapters, we now turn to molecular designs which seek to overcome the effects of chain collapse by clustering associating groups at the end of polymer chains (Figure 1.7.3 and 1.7.4).

3.5 Figures, Schemes, and Tables

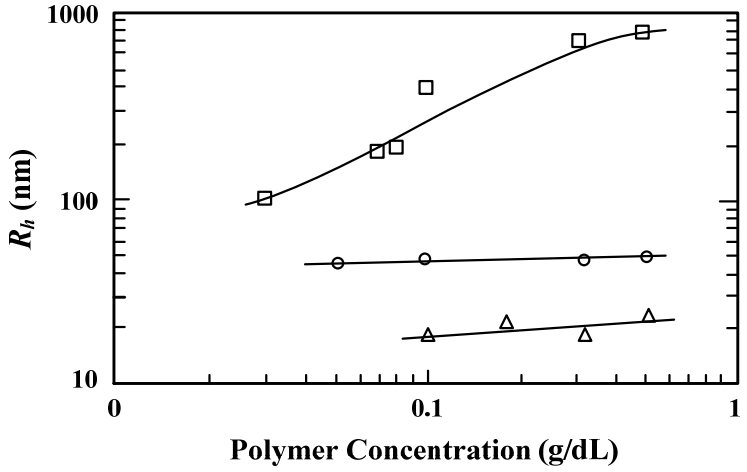

Figure 3.1 Hydrodynamic radii of proton-donating polymer DAMA, proton-accepting polymer PSDAVP, and their mixture (1:1 ratio by weight) in kerosene. The overlap concentration of the chains corresponds to $c^* = 0.3$ g/dL for PSDAVP and $c^* = 0.7$ g/dL for DAMA. (Adapted from Malik and Mashelkar[3] and reproduced with permission.)

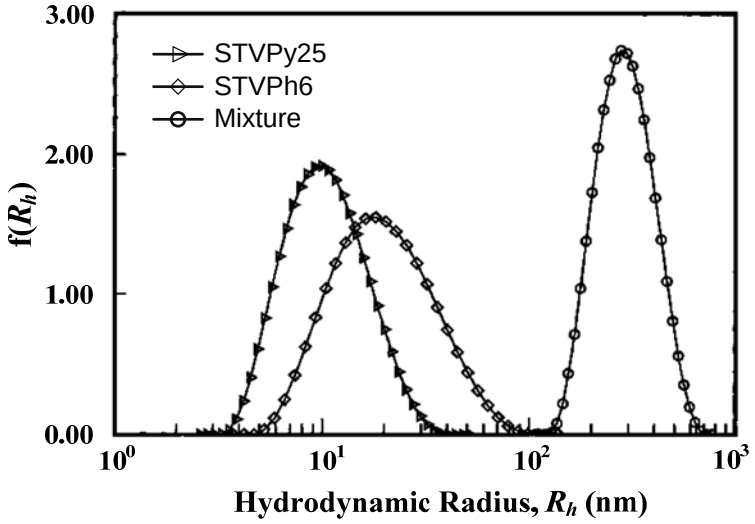

Figure 3.2 Hydrodynamic radius distribution f(R_h) of proton-donating and proton-accepting polymers containing 6 and 25 mol % vinyl phenol and vinyl pyridine monomers, and their mixture (1:1 ratio by weight) in butanone. Measurements were conducted at scattering angle of 15^o for solutions of total polymer concentration 1×10^{-4} g/mL. (Adapted from Xiang et al.[4] and reproduced with permission.)

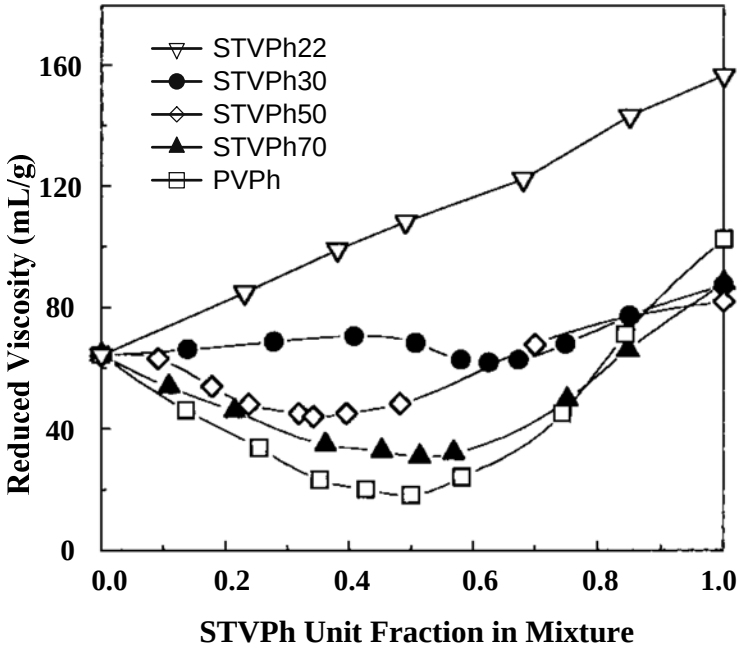

Figure 3.3 Reduced viscosity ($\eta_r = \eta_{sp}/c$, at total polymer concentration c = 1.5 mg/mL) of mixtures of STVPy containing 25% vinyl pyridine monomers and STVPh containing 22-100% vinyl phenol monomers in THF as a function of the unit fraction of STVPh, i.e., the fraction of monomers in solution that belong to STVPh molecules. (Adapted from Xiang et al.[4] and reproduced with permission.)

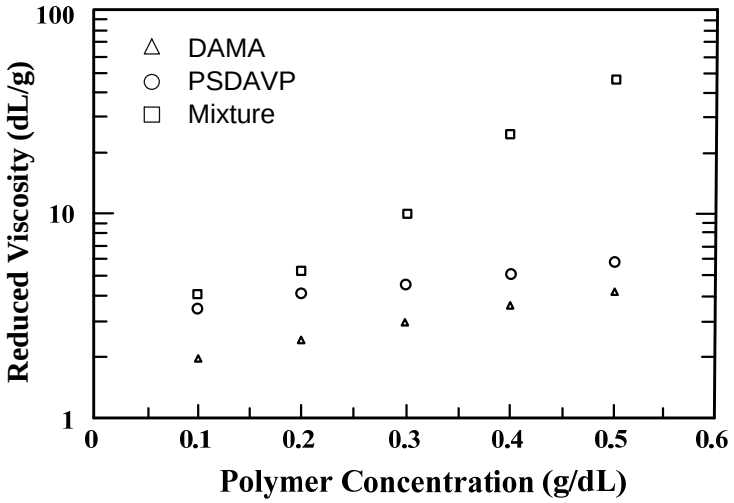

Figure 3.4 Reduced viscosity vs. concentration for proton-donating polymer DAMA, proton-accepting polymer PSDAVP, and their mixture (1:1 ratio by weight) in kerosene, showing that interpolymer associations result in a non-linear increase of viscosity with concentration even at dilute concentrations. The overlap concentration of the chains corresponds to $c^* = 0.3$ g/dL for PSDAVP and $c^* = 0.7$ g/dL for DAMA. (Adapted from Malik and Mashelkar[3] and reproduced with permission.)

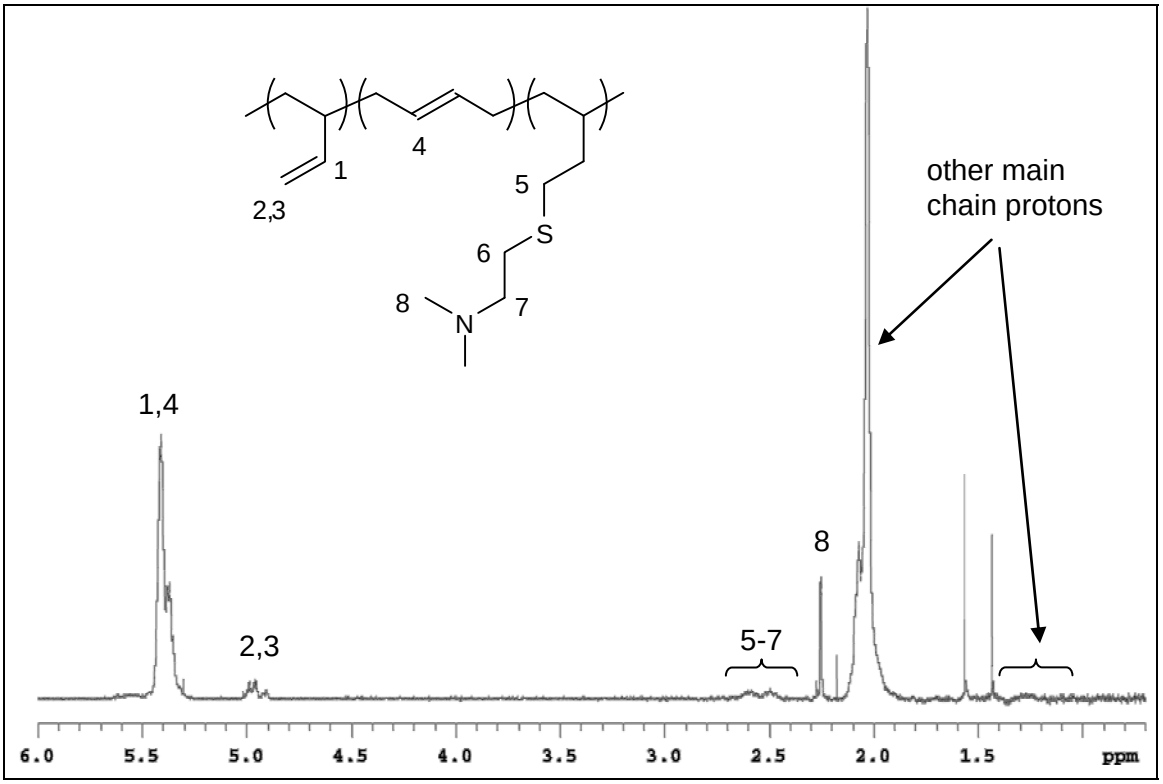

Figure 3.5. Representative ^{1}H NMR spectrum of 1250 kg/mol 1,4-polybutadiene polymer functionalized with 2-(dimethylamino)ethane thiol (1250PB2.6N, refer to Table 3.1). Visible peaks at δ = 2.27 ppm and 1.43 ppm belong to 2,6-ditertbutyl-4-methylphenol (BHT), and the peak near $\delta \sim 1.6$ ppm corresponds to water.

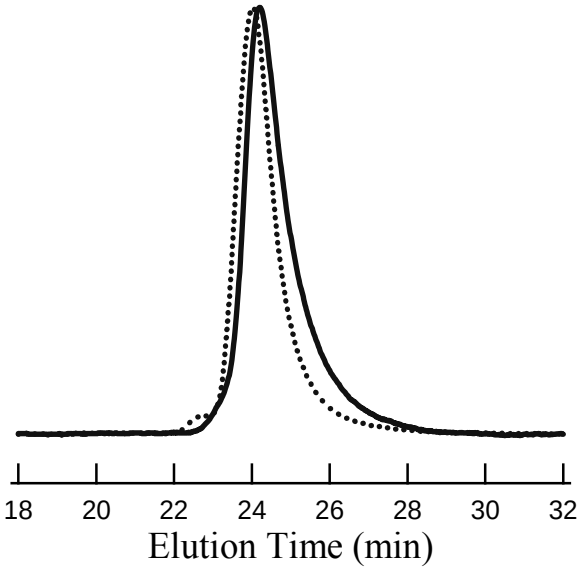

Figure 3.6 Representative gel permeation chromatography (GPC) trace of 1,2-polybutadiene functionalized with DMAET. The dashed line is 510 kg/mol 1,2-PB prepolymer; the solid line corresponds to 510kPB1.6N polymer (refer to Table 3.2) after > 2 years of storage, during which a slight broadening to the right of the size distribution curve was observed to have occurred.

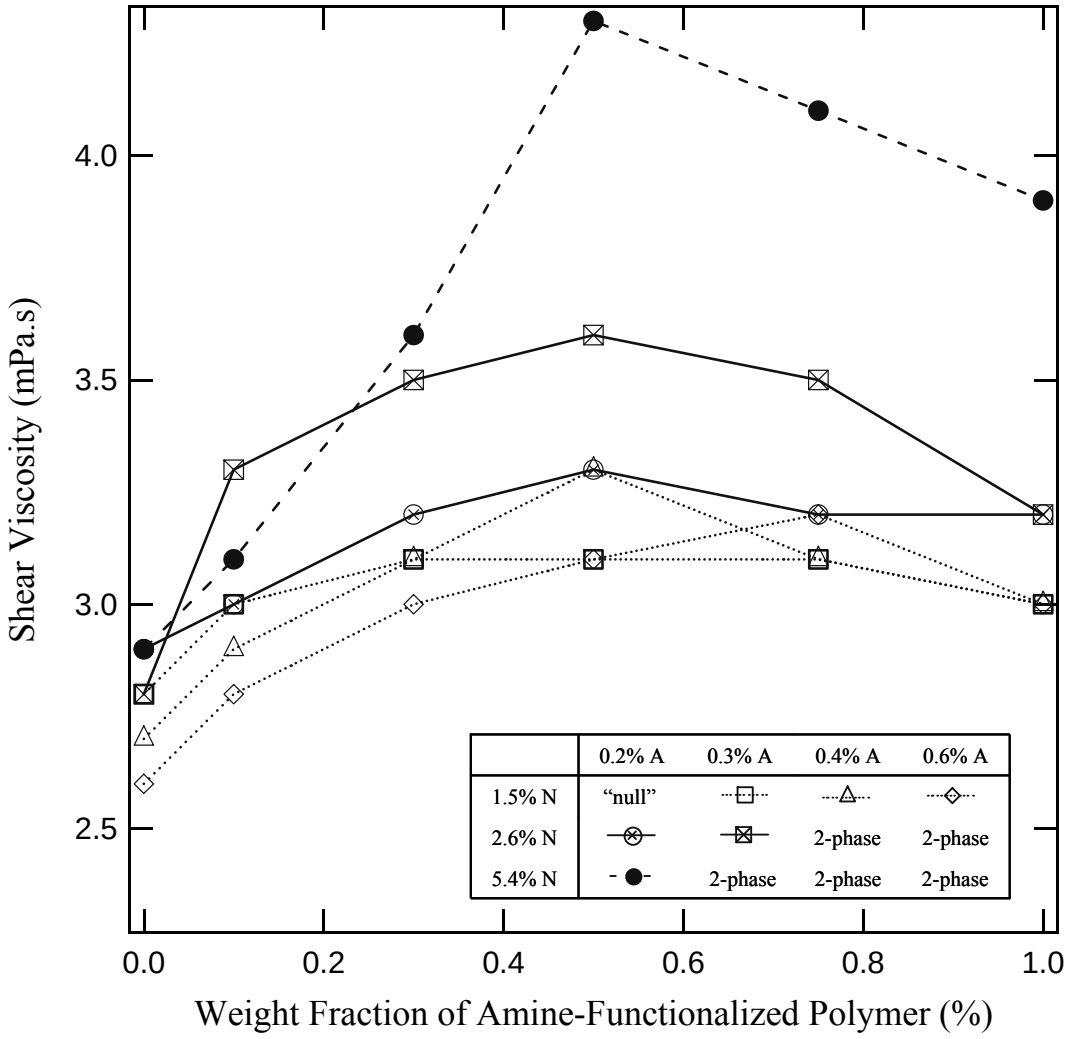

Figure 3.7 Shear viscosity of mixtures of proton-donating (1250kPBxxA) and proton-accepting (1250kPBxxN) chains in Jet-A at total polymer wt fraction of 2500 ppm, as a function of the fraction (wt 1250kPBxxN)/(wt 1250kPBxxN + wt 1250kPBxxA). The viscosities of the solvent and of the 1250k 1,4-PB prepolymer at 2500 ppm in Jet-A were 1.43 and 3.0 mPa.s, respectively.

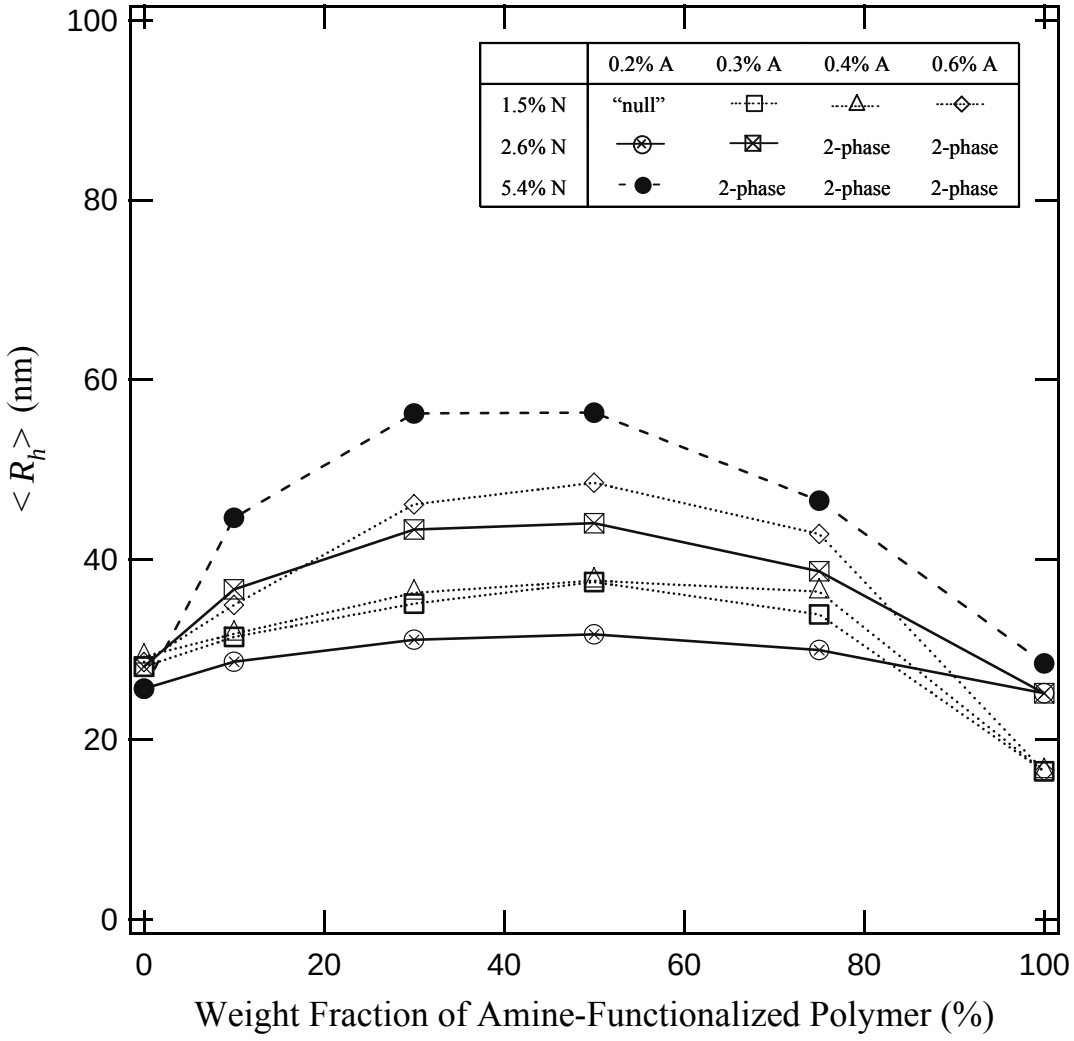

Figure 3.8 Hydrodynamic radii of mixtures of proton-donating (1250kPBxxA) and proton-accepting (1250kPBxxN) chains in Jet-A at total polymer wt fraction of 1500 ppm, as a function of the fraction (wt 1250kPBxxN)/(wt 1250kPBxxN + wt 1250kPBxxA).

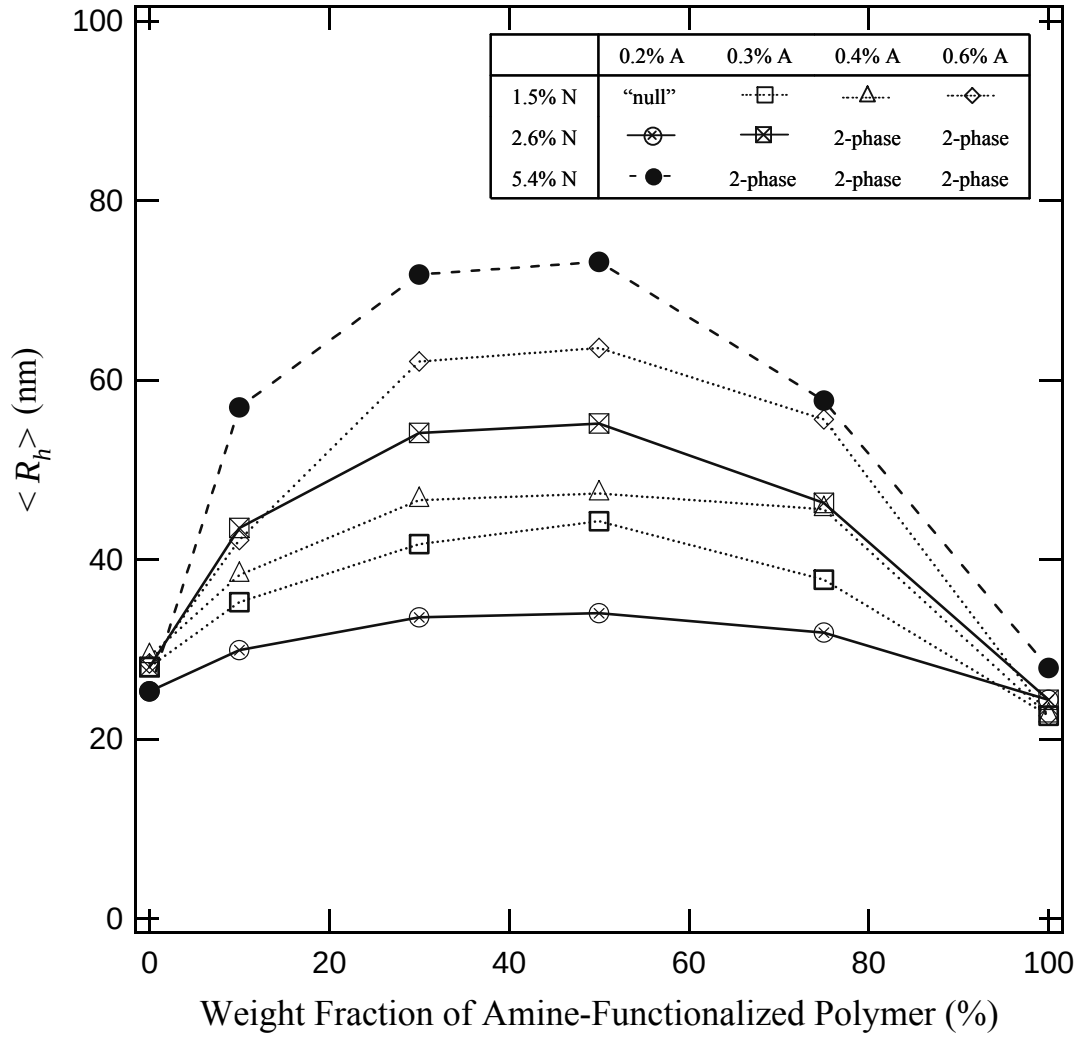

Figure 3.9 Hydrodynamic radii of mixtures of proton-donating (1250kPBxxA) and proton-accepting (1250kPBxxN) chains in Jet-A at total polymer wt fraction of 2500 ppm, as a function of the fraction (wt 1250kPBxxN)/(wt 1250kPBxxN + wt 1250kPBxxA).

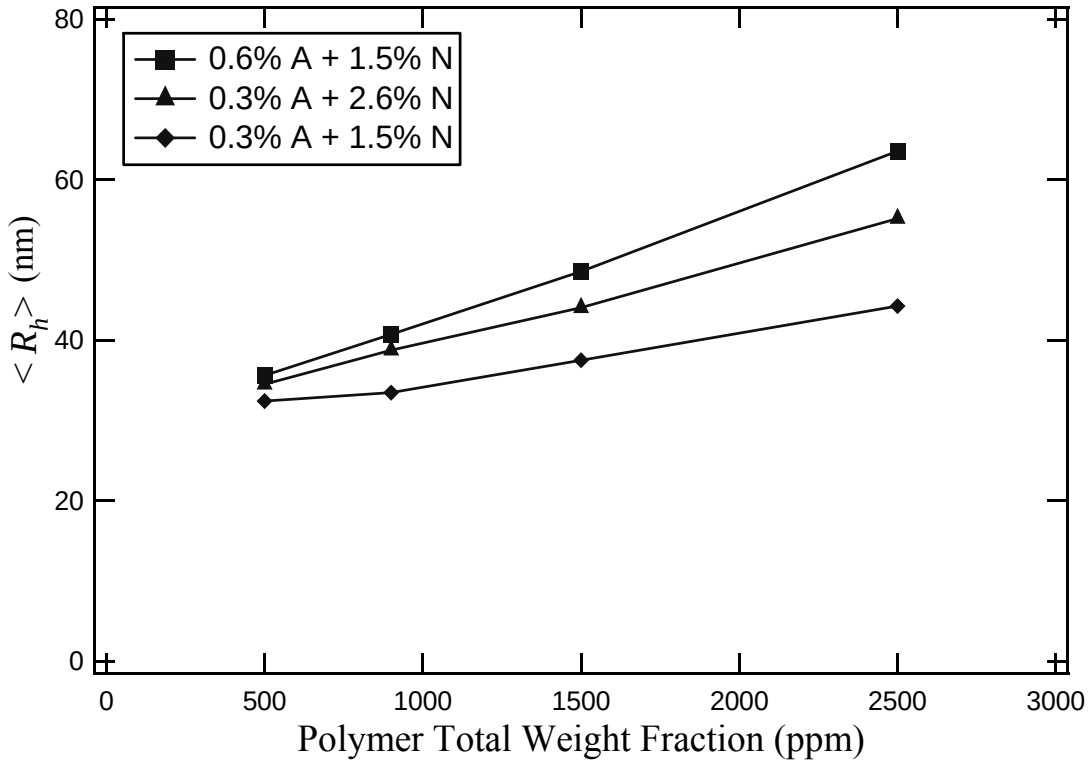

Figure 3.10 Hydrodynamic radii of mixtures of proton-donating (1250kPBxxA) and proton-accepting (1250kPBxxN) chains in 1:1 wt ratio in Jet-A, as a function of increasing total polymer concentration in the dilute regime.

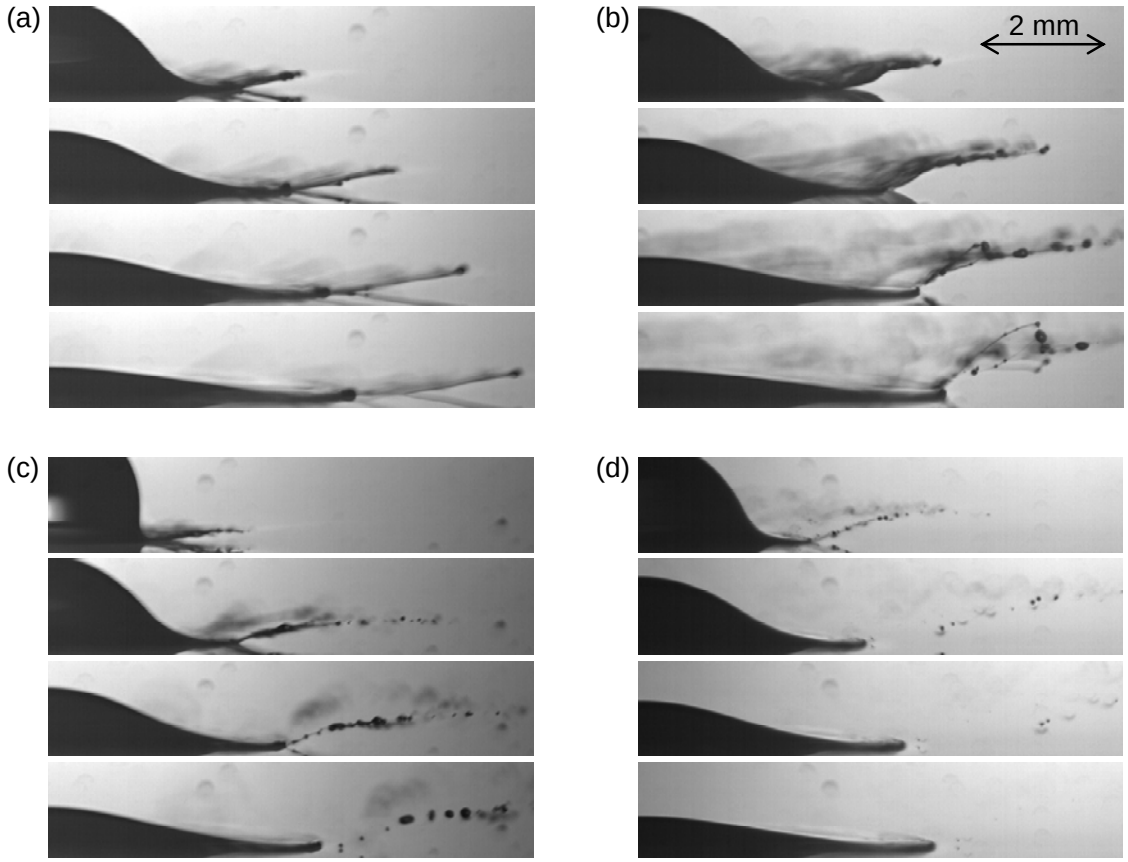

Figure 3.11 High-speed imaging of drop breakup of polymer solutions at 180 ppm by wt in Jet-A: (a) 4200 kg/mol linear, non-associating polyisobutylene chains; (b) 1250 kg/mol linear, unfunctionalized 1,4-polybutadiene (PB) chains; (c) 1250kPB0.3A and 1250kPB2.6N in 3:1 wt ratio; and (d) 1250kPB0.3A and 1250kPB2.6N in 1:1 wt ratio (refer to Table 3.1). For 4200 kg/mol polyisobutylene, satellite droplets were never fully ejected; on the other hand all visible fluid filaments connecting "beads" of fluid together had broken 2 ms, 1 ms, and 0.5 ms after impact for solutions b, c, and d, respectively. The interval between frames is 0.25 ms in all cases.

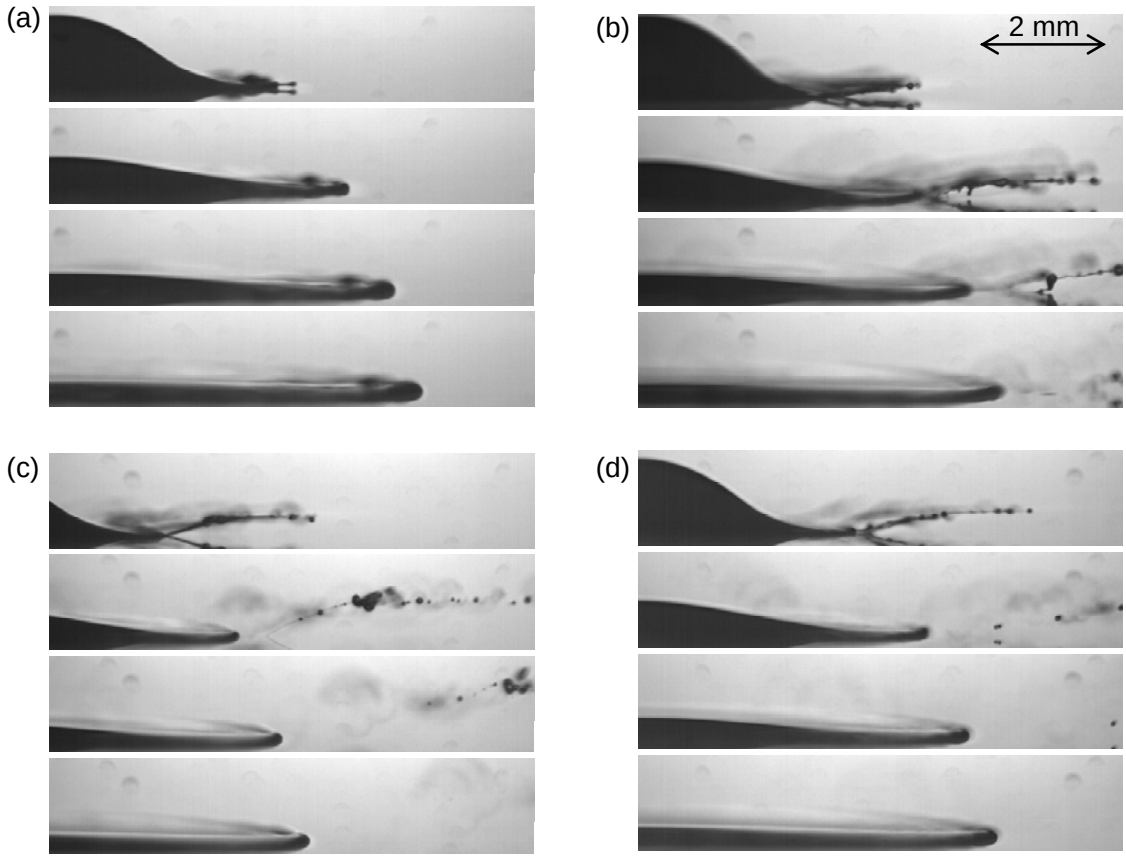

Figure 3.12 High-speed imaging of drop breakup of polymer solutions at 450 ppm by wt in Jet-A: (a) 4200 kg/mol linear, non-associating polyisobutylene chains; (b) 1250 kg/mol linear, unfunctionalized 1,4-polybutadiene (PB) chains; (c) 1250kPB0.3A and 1250kPB2.6N in 3:1 wt ratio; and (d) 1250kPB0.3A and 1250kPB2.6N in 1:1 wt ratio (refer to Table 3.1). For 4200 kg/mol polyisobutylene, there is nearly complete suppression of breakup without formation of satellite droplets; on the other hand all visible fluid filaments connecting "beads" of fluid together had broken 2.5 ms, 1.25 ms, and 0.75 ms after impact for solutions b, c, and d, respectively. The interval between frames is 0.5 ms in all cases.

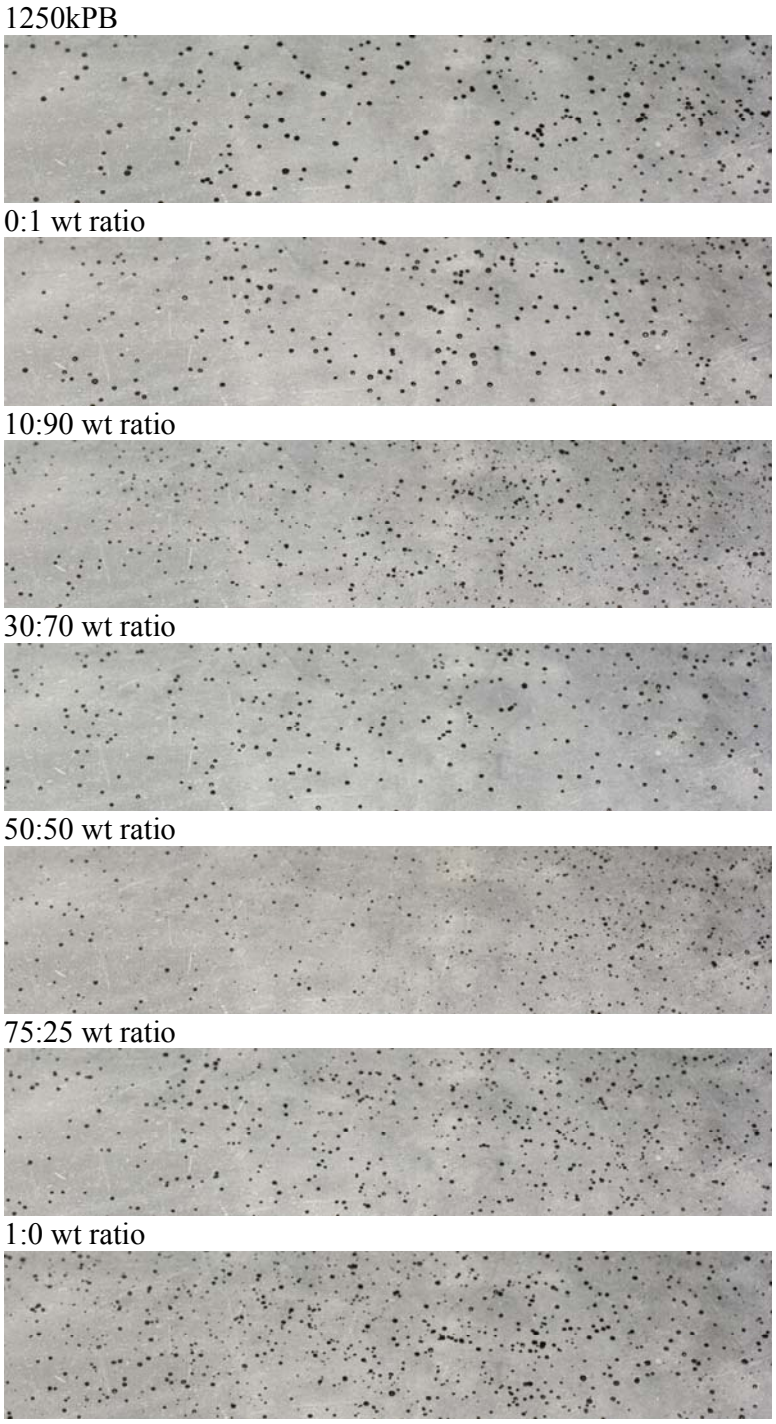

Figure 3.13 Mixture of 1250kPB0.6A and 1250kPB1.5N polymers at total concentration of 2500 ppm by wt in Jet-A, as a function of increasing wt ratio of 1250kPB1.5N to 1250kPB0.6A polymers. The top image corresponds to a reference solution of 1250kPB prepolymer.

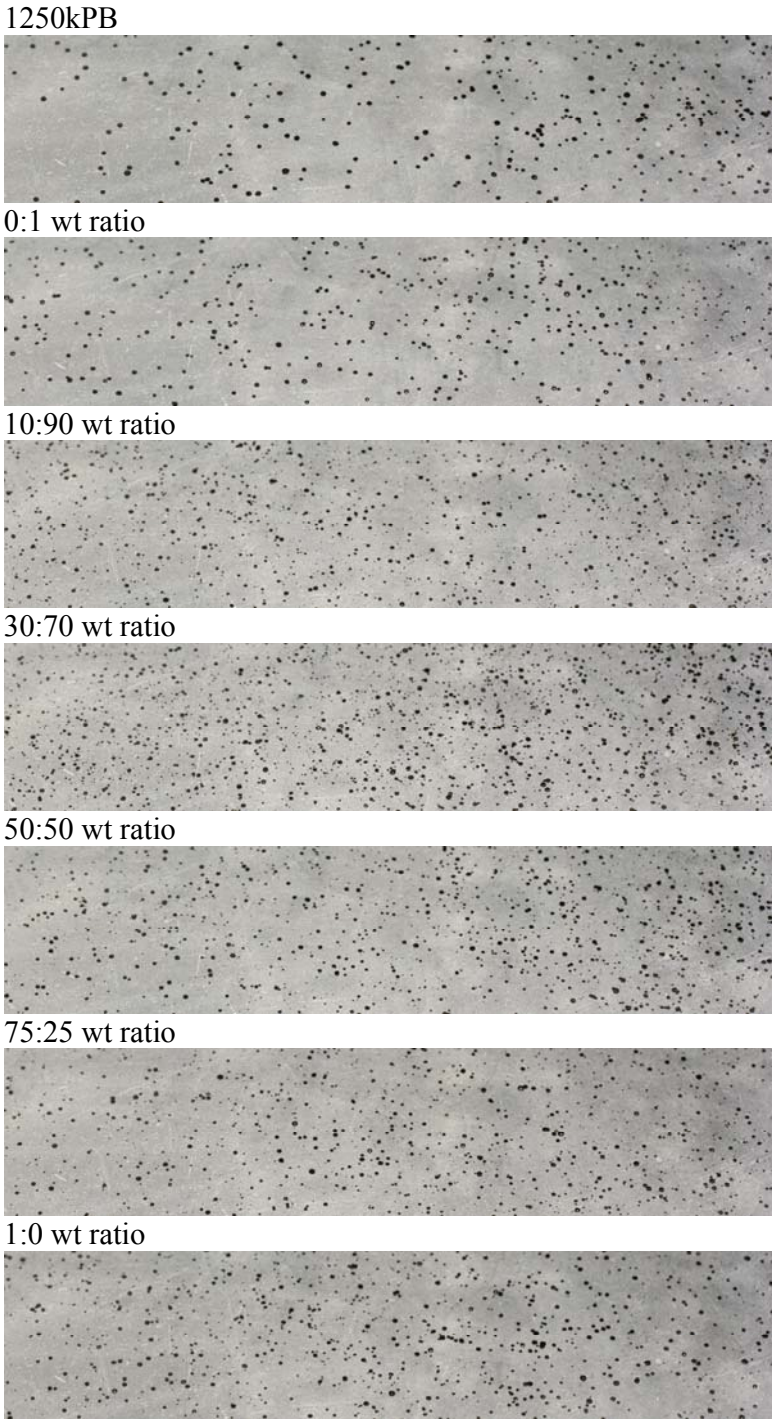

Figure 3.14 Mixture of 1250kPB0.4A and 1250kPB1.5N polymers at total concentration of 2500 ppm by wt in Jet-A, as a function of increasing wt ratio of 1250kPB1.5N to 1250kPB0.6A polymers. The top image corresponds to a reference solution of 1250kPB prepolymer.

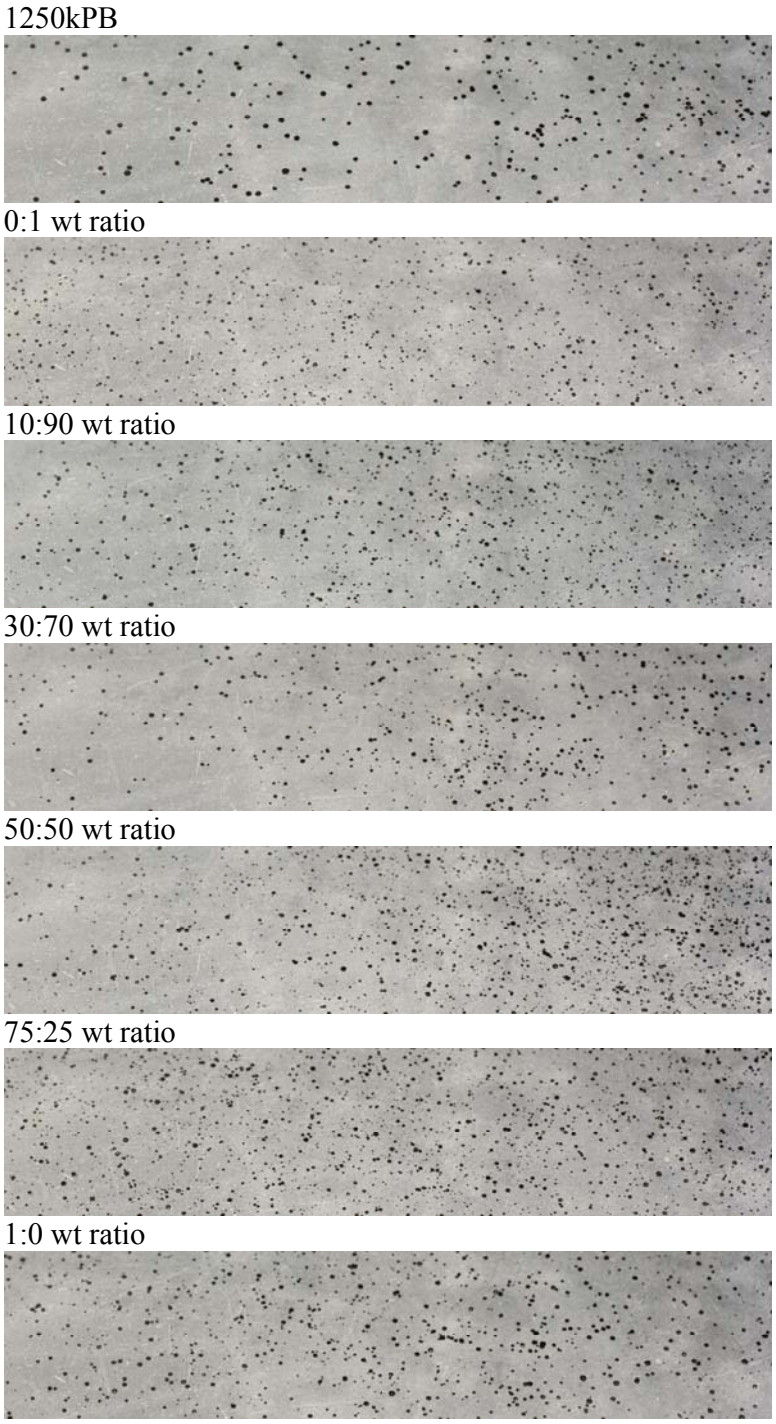

Figure 3.15 Mixture of 1250kPB0.3A and 1250kPB1.5N polymers at total concentration of 2500 ppm by wt in Jet-A, as a function of increasing wt ratio of 1250kPB1.5N to 1250kPB0.6A polymers. The top image corresponds to a reference solution of 1250kPB prepolymer.

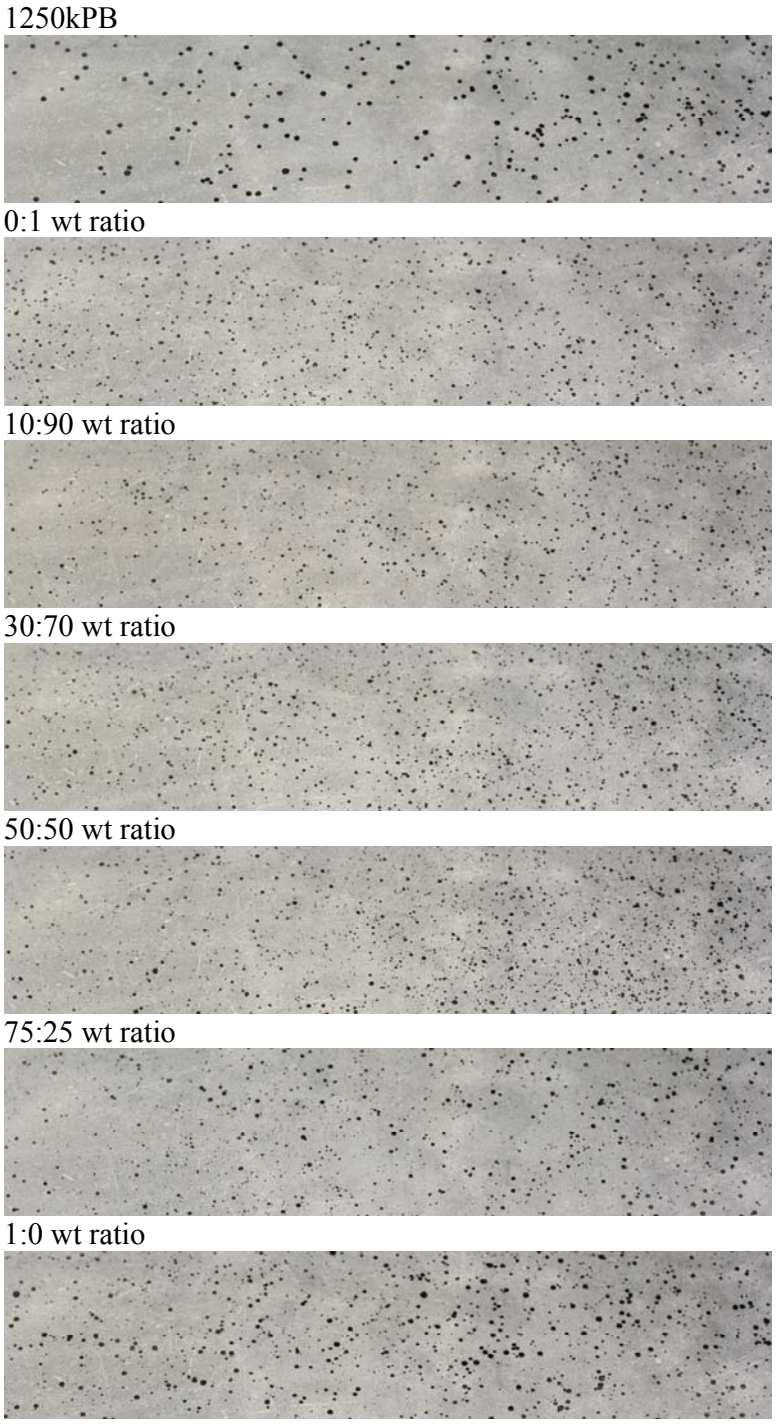

Figure 3.16 Mixture of 1250kPB0.3A and 1250kPB2.6N polymers at total concentration of 2500 ppm by wt in Jet-A, as a function of increasing wt ratio of 1250kPB1.5N to 1250kPB0.6A polymers. The top image corresponds to a reference solution of 1250kPB prepolymer.

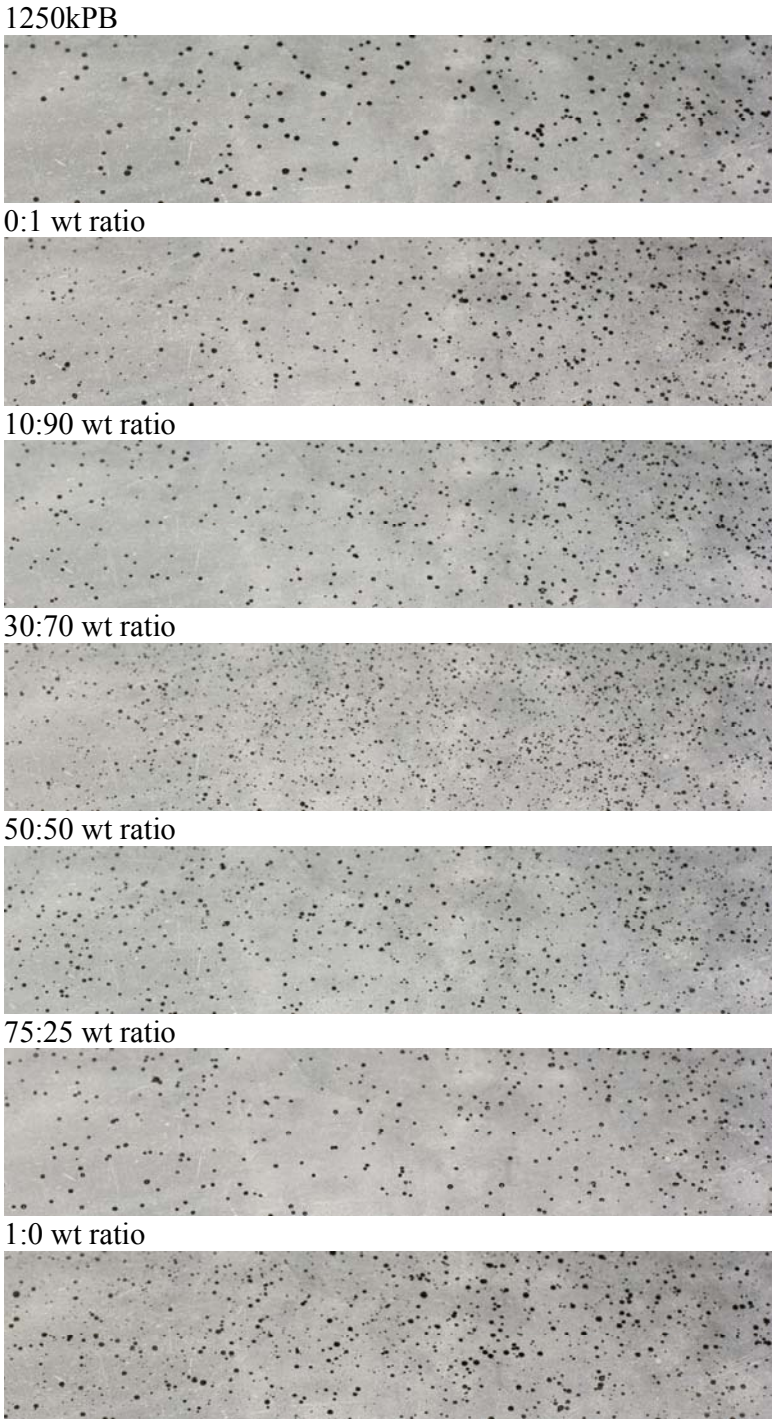

Figure 3.17 Mixture of 1250kPB0.2A and 1250kPB2.6N polymers at total concentration of 2500 ppm by wt in Jet-A, as a function of increasing wt ratio of 1250kPB1.5N to 1250kPB0.6A polymers. The top image corresponds to a reference solution of 1250kPB prepolymer.

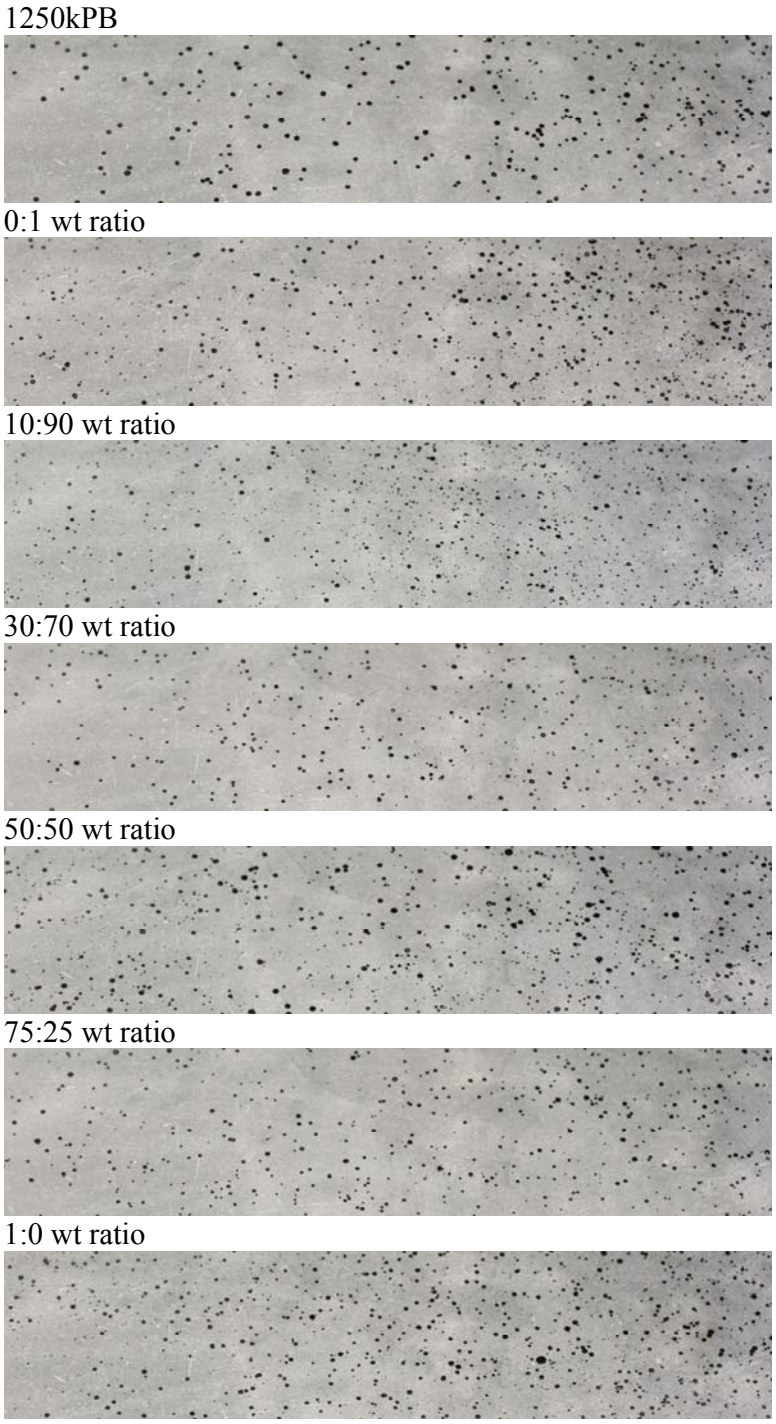

Figure 3.18 Mixture of 1250kPB0.2A and 1250kPB5.4N polymers at total concentration of 2500 ppm by wt in Jet-A, as a function of increasing wt ratio of 1250kPB1.5N to 1250kPB0.6A polymers. The top image corresponds to a reference solution of 1250kPB prepolymer.

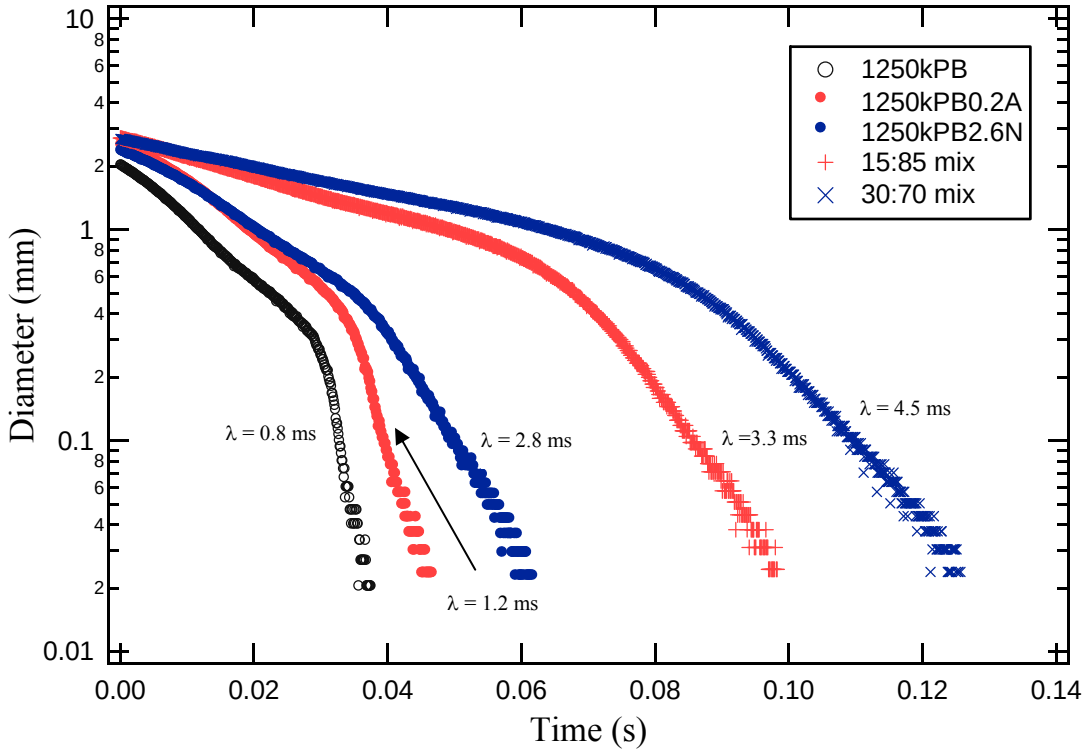

Figure 3.19 Time evolution of filament diameter during capillary breakup experiments for mixtures of 1250k2.6N and 1250k0.2A polymers in 15:85 and 30:70 wt ratios, and for appropriate reference solutions, at 1.5 wt % total polymer content in Jet-A (corresponding to $c = 6c^*$ for 1250kPB prepolymer). All tests were performed with 8 mm diameter plates, at initial and final aspect ratios of 1.0 and 2.2, respectively. Solution shear viscosities were 48 mPa.s, 62 mPa.s, and 77 mPa.s for the 1250kPB, 1250kPB0.2A, and 1250kPB2.6N reference solutions, and 130 mPa.s and 180 mPa.s for the 85:15 and 70:30 mixtures, respectively. The characteristic relaxation times of the solutions, determined from the slope of the exponential decay of the filament diameter vs. time, are represented on the figure.

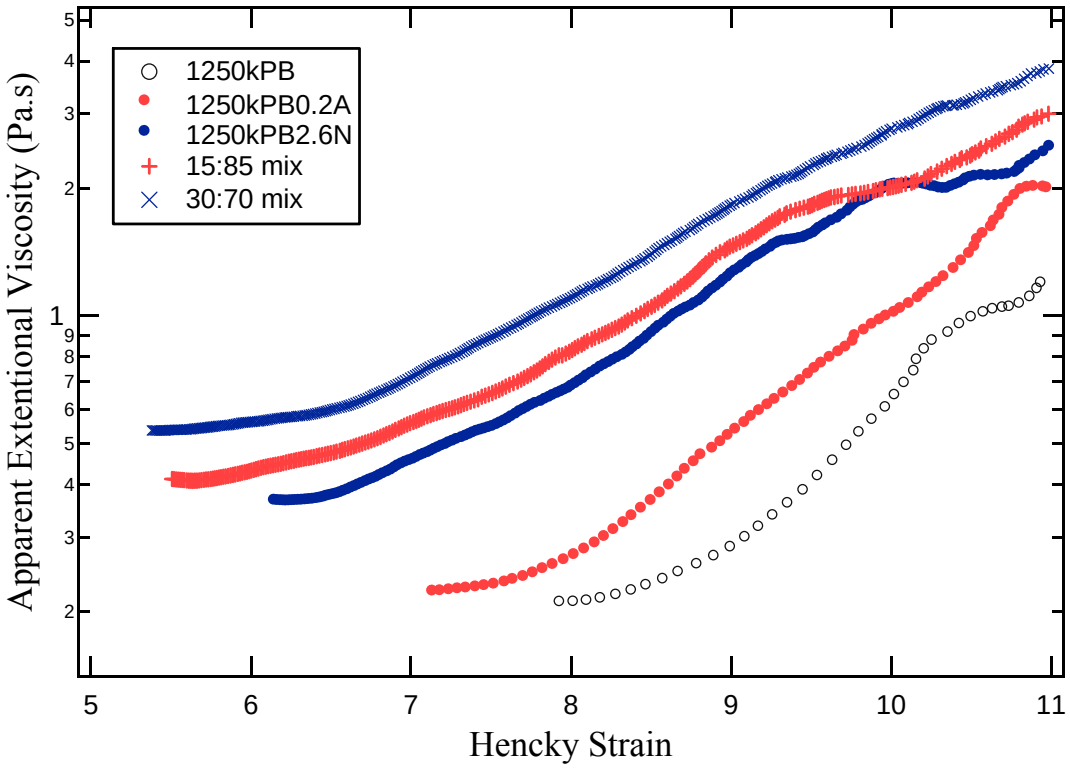

Figure 3.20 Effect of acid-base complementary associations on apparent extentional viscosity during capillary breakup rheology (refer to Figure 3.19 for experimental details).

Scheme 3.1 Preparation of Functionalized 1250 kg/mol 1,4-Polybutadiene Molecules Used in the Present Study: Thiol-Ene Addition of (a) 3-Mercaptopropionic Acid, and (b) Dimethylaminoethanethiol Hydrochloride

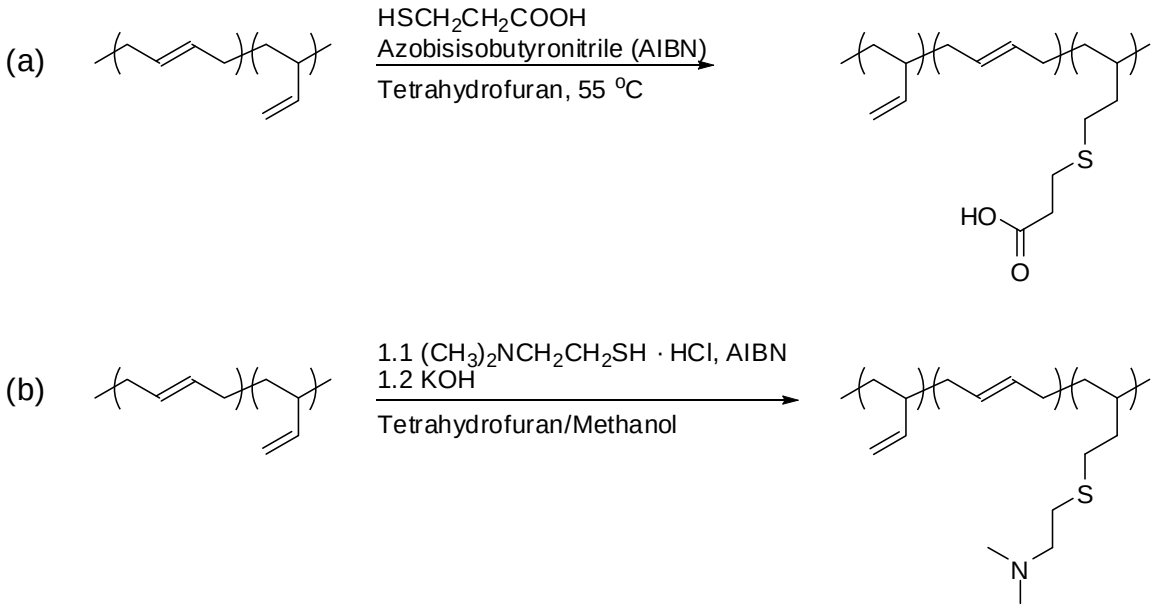

Table 3.1 Reaction Conditions[a] and Results for Functionalization of 1250 kg/mol 1,4-Polybutadiene

Entry[b]	[PB] (g/mL)	[RSH][c]	[AIBN] (mg/mL)	Rxn time (hrs)	Funct.[d] %	PDI[e]
1250kPB1.5N	0.008	2.8	0.86	7.0	1.5	-
1250kPB2.6N[f]	0.011	13	1.1	11[h]	2.6	-
1250kPB5.4N	0.009	20	1.1	12[i]	5.4	-
1250kPB0.2A[g]	0.010	12	0.46	0.58	0.2	1.15
1250kPB0.3A	0.009	16	0.62	0.55	0.3	1.29
1250kPB0.4A	0.009	16	0.52	1.1	0.4	1.17
1250kPB0.6A	0.009	16	0.54	1.2	0.6	1.23

[a]In all cases, reactions were run in THF for functionalization with MPA, and ~ 9:1 THF: methanol for functionalization with DMAET. [b]Functionalized PB polymers were named so that the prefix corresponds to the molecular weight of the precursor chain, and the suffix represents the mol % of monomers bearing functional groups (abbreviated as N for DMAET and A for MPA). [c]In molar equivalent of 1,2-PB units, which are 98% of the units of 510kPB and 8% of the units of 1250kPB. [d]Molar fraction of functionalized monomers based on the total number of PB monomers (both 1,2 and 1,4 units). [e]The 1250kPB prepolymer had a PDI value of 1.09. [f] ^{1}H NMR spectrum shown in Figure 3.5. [g]GPC trace given in Figure 2.4. [h]Reaction temperature was 50 ºC instead of 55 ºC. [i]First 9 hrs at 55 ºC and last 3 hrs at 65 ºC.

Table 3.2 Reaction Conditions[a] and Results for Functionalization of 510 kg/mol 1,2-Polybutadiene

Entry[b]	PB (g)	RSH[c]	AIBN (mg)	Rxn time (hrs)	Funct.[d] %	PDI[e]
510kPB1.6N[f]	0.55	3.9%	11	1.1	1.6	~ 1.2
510kPB4.0N	0.54	9.5%	10	1.1	4.0	~ 1.2
510kPB6.6N	~ 0.3	~ 20%	~ 10	~ 1	6.6	~ 1.2

[a]In all cases, reactions were run in 30 mL of a mixture of THF and methanol in 9:1 volume ratio. [b]Functionalized PB polymers were named as described in the footnote of Table 3.1. [c]In molar equivalent of 1,2-PB units. [d]Molar fraction of functionalized monomers. [e]The 510kPB prepolymer had a PDI value of 1.15. [f]GPC trace given in Figure 3.6.

Table 3.3 Phase Behavior[a] of Mixtures of 1250kPB Proton-Donating and Proton-Accepting Chains in Jet-A Solvent

	0.2% A[b]	0.3% A	0.4% A	0.6% A
1.5% N[c]				
2.6% N				
5.4% N				

[a]Shaded boxes correspond to phase separated mixtures, at 25 ºC and total polymer concentrations of 0.25 wt %. [b]The degree of functionalization with 3-mercaptopropionic acid. [c]The degree of functionalization with 2-(dimethylamino)ethanethiol.

Table 3.4 Summary of Experiments[a] Conducted on Mixtures of 1250kPB Proton-Donating and Proton-Accepting Chains in Jet-A Solvent

	0.2% A[b]	0.3% A	0.4% A	0.6% A
1.5% N[c]				
2.6% N	**CaBER**	**Drop Breakup**		
5.4% N				

[a]Shaded boxes correspond to mixtures for which spray experiments, as well as shear viscosity and size measurements were made for solutions at 25 ºC and total polymer concentrations of 0.25 wt %. [b]The degree of functionalization with 3-mercaptopropionic acid. [c]The degree of functionalization with 2-(dimethylamino)ethanethiol.

3.6 References and Notes

1. Kowalik, R. M.; Duvdevani, I.; Peiffer, D. G.; Lundberg, R. D.; Kitano, K.; Schulz, D. N., Enhanced drag reduction via interpolymer associations. *Journal of Non-Newtonian Fluid Mechanics* **1987,** 24, (1), 1–10.

2. Refer to Chapter 1, Section 1.2.2. Malik and Mashelkar (see reference 3 below) reported that interpolymer complexation resulted in large aggregates with drag-reduction activity up to 6 times greater than that of non-associating counterparts, and further that interpolymer complexation increased shear-stability of the polymer components compared to the stability of the individual components by themselves.

3. Malik, S.; Mashelkar, R. A., Hydrogen-bonding mediated shear stable clusters as drag reducers. *Chemical Engineering Science* **1995,** 50, (1), 105–116.

4. Xiang, M. L.; Jiang, M.; Zhang, Y. B.; Wu, C.; Feng, L. X., Intermacromolecular complexation due to specific interactions .4. The hydrogen-bonding complex of vinylphenol-containing copolymer and vinylpyridine-containing copolymer. *Macromolecules* **1997,** 30, (8), 2313–2319.

5. Qi, G. R.; Wang, Y. H.; Li, X. X.; Peng, H. Y.; Yang, S. L., Viscometric study on the specific interaction between proton-donating polymers and proton-accepting polymers. *Journal of Applied Polymer Science* **2002,** 85, (2), 415–421.

6. Wang, Y. H.; Qi, G. R.; Li, H. L.; Yang, S. L., Effect of chain compositions on interpolymer specific interaction in solutions. *European Polymer Journal* **2002,** 38, (7), 1391–1397.

7. Wang, Y. H.; Qi, G. R.; Peng, H. Y.; Yang, S. L., Interpolymer specific interaction in blends of poly(styrene-co-alkyl acrylate-co-4-vinylpyridine) and poly(styrene-co-alkyl acrylate-co-acrylic acid). *Polymer* **2002,** 43, (9), 2811–2818.

8. Qiu, X. P.; Jiang, M., Intermacromolecular complexation due to specific interactions .1. The hydrogen-bonding complex between poly(methyl methacrylate) and modified polystyrene. *Polymer* **1994,** 35, (23), 5084–5090.

9. Qiu, X. P.; Jiang, M., Intermacromolecular complexation due to specific interactions .3. Miscibility and complexation of Pbma and Ps(Oh). *Polymer* **1995,** 36, (18), 3601–3604.

10. Refer to Section 2.3.2

11. Yu, J. H.; Fridrikh, S. V.; Rutledge, G. C., The role of elasticity in the formation of electrospun fibers. *Polymer* **2006,** 47, (13), 4789–4797.

12. Refer to Section 2.3.6.1

13. Attempts were made, without success, to make capillary breakup measurements of dilute 1250 kg/mol PB chains in a solvent of enhanced shear viscosity, such as Jet-A containing 3–15 wt % 50–500 kg/mol polyisobutylene or polyisoprene chains. In all such attempts solution shear viscosity was still too low to enable elasticity measurements of the 1250 kg/mol PB solutions, or the 1250 kg/mol PB chains phase separated.

14. Schulz, D. N.; Kitano, K.; Duvdevani, I.; Kowalik, R. M.; Eckert, J. A., Hydrocarbon-soluble associating polymers as antimisting and drag-reducing agents. *ACS Symposium Series* **1991,** 462, 176–189.